University of Sistan and Baluchestan

Challenges in Nano and Micro Scale Science and Technology

Online ISSN: 2821 - 000X

Thermal Simulation of Microencapsulate Phase Change Materials in an Energy Storage Based on Palmitic Acid

Hossein Pourmohamadian

Department of Mechanical, Nar. C., Islamic Azad University, Naragh, Iran. Email: Pmohamadian@iau.ac.ir

Article Info

Article type:
Research Article

Keywords:
phase change material,
palmitic acid,
microcapsule,
energy storage,
thermal simulation,

ABSTRACT

Phase change materials (PCM) can be employed in many fields due to their capacity to absorb and release energy when it is necessary. Nowadays, the number of studies about these kinds' materials is increasing because of their benefits in the energy storage systems. In microencapsulation, the core material is defined as the specific material coated and can be in the liquid or solid state depending on the temperature. In this research, two new PCM microcapsules based on palmitic acid (PA) core and silicon dioxide (SiO_2), strontium titanate ($SrTiO_3$) were shelled and synthesized through self-method in three core/shell weight ratios (50/50, 40/60, 30/70). Finding the thermal properties of these materials experimentally, then the thermal simulation in rectangular energy storage was performed under thermal flux. The simulated results were analyzed and discussed. Among the synthesized microcapsules, the best results were PA@SiO_2 with a weight ratio of 30/70. This sample had maximum amount of 24.42% melting time in 12,000 seconds and the maximum temperature at 369 K, which indicated 196.8% higher than the pure PA.

Nomenclature

C_p	specific heat (J/kg K)
E	calibration constant of DSC
f	local melting fraction
H	total energy (J/m^3)
h	enthalpy of sensible heat (J/m^3)
k	thermal conductivity (W/m K)
L	latent heat (J/m^3)
q	heat flux
S	source term
T	temperature (K, ºC)
t	time (s)
v	velocity (m/s)
X	melting front position to the right side wall (m)

Greek letter

ρ	density
$\emptyset_v$	volume fraction
$\emptyset_w$	weight fraction

Subscript

c	continuous
d	discrete
eff	effective
f	solid state
m	melting state

Abbreviation

DSC	Differential Scanning Calorimeter
FT-IR	Fourier Transform of Infrared spectroscopy
MPCM	Microcapsulated PCM
PA	Palmitic acid
PA@SiO_2	Palmitic acid is core and SiO_2 is shell
PA@$SrTiO_3$	Palmitic acid is core and $SrTiO_3$ is shell
PCM	Phase Change Material
SEM	Scanning Electron Microscope
TEM	Transmission Electron Microscope
TGA	Thermal Gravimetric Analysis
TES	Thermal Energy Storage
XRD	X-Ray Diffraction

INTRODUCTION

Thermal energy storage latent in the phase-change materials is a method that has been widely studied in recent decades.[1] Theoretical and experimental studies have been carried out on the thermal energy storage of phase change materials (PCMs) in various geometries [2].

Guan et al. review recent advances in phase change materials (PCM) for thermal energy storage,[3] and Li et al. introduce new phase change materials and analyze their applications, especially in the field of buildings.[4] Zhang et al. review the thermal performance of PCMs, discuss their advantages and disadvantages, and also examine their

How to Cite this paper: Pourmohamadian H. Thermal Simulation of Microencapsulate Phase Change Materials in an Energy Storage Based on Palmitic Acid. *Challenges in Nano and Micro Scale Science and Technology*. 2024; 12(1): 40-47. DOI: 10.22111/cnmst.2025.50355.1255

© Pourmohamadian H. Publisher: University of Sistan and Baluchestan.

DOI: 10.22111/cnmst.2025.50355.1255

impact on energy efficiency.[5] In addition, Khan et al. review innovative PCMs for building applications and their role in optimizing energy consumption,[6] and Charmes et al. provide insights into recent developments and future prospects of this technology.[7]

Encapsulating is the process of putting solids or droplets of liquids or gases in with a compatible thin solid wall. The substance is filled inside the capsule as a core or internal phase, while the wall is sometimes called a shell, cover, or membrane. Typically, packaged materials are classified as nanocapsules, microcapsules and macrocapsules based on the capsule diameter. The diameter of the microcapsules varies from 1mm to 1μm, while capsules smaller than 1μm are classified as nanocapsules and larger than 1μm as macrocapsules [8].

Over time, the technology of encapsulation in many fields were progressed, e.g. the pharmaceutical industry [9], cosmetics [10], packaging of phase change material for thermal energy storage [11], textile industries [12], and food [13].

At present, there are several solutions for constracting stable PCM composites,[14] including the use of supporting materials for PCMs such as polymers or porous materials to form stable composites or encapsulate PCMs [15].

The encapsulation of PCMs into inert materials is the most effective and in fact the most beneficial way to prepare form-stablePCMs. This method can be in the form of putting solid or liquid particles in a solid wall. Therefore, it can reduce the leakage of PCM from their location, reduce the interference in the phase change behavior from the outside environment, increase the heat transfer surface area, and control PCMs of the liquid during the phase change process [16].

In the past, the microcapsulation method of PCMs was performed using polymeric wall materials such as melamine formaldehyde resins, urea-formaldehyde resins, polyurethanes, polystyrene, styrene-butadiene-styrene copolymer, poly (methyl methacrylate) and through polymerization in an emulsion system. In general, these microcapsules have shown a shell-cell structure with beneficial effects [17]. However, several defects such as flammability, poor thermal properties and poor chemical stability and low thermal conductivity for this type of microcapsules packaging are due to polymeric shells [18, 19]. Studies carried out by Sukhorukov et al. [20] and Jamekhorshid et al. [21] indicated that the size of PCMs is very important since the microencapsulation of PCMs in nanoscales is much more stable than microencapsulation of PCM in microscale. They observed that the mechanical deformation of microencapsulation of PCMs at 10nm was much less, than the microencapsulations of PCMs at 10μm. In addition, the compatibility of plastics with PCMs is a key point. Castellon et al. [22] studies show that low-density polyethylene and polypropylene have the worst behavior in comparison with high-density polyethylene for PCM encapsulation. Since the main problem with passive systems is the leakage of compressed microcapsules inside the wall in a building, Giro-Paloma et al. [23] investigated hardness and Young's modulus of different polymers.

Kuznik et al. [24] have shown three characteristics for assessing the microencapsulation quality of PCMs, which include the average diameter, shell thickness, and mass fraction of PCM in comparison with the total mass of the capsule.

The thermal conductivity of minerals is usually higher than organic materials. In addition, the resistance to fire, as well as the chemical and thermal stability of minerals is better than the organic materials [25].

Therefore, recent efforts have been made to increase the thermal conductivity and mechanical strength of microcapsules by microencapsulation of PCMs with mineral shells. Wang et al. [26] have reported the method for the preparation of microcapsules with silica in an oil-in-water emulsion. Zhang et al. [27] used a sol-gel method to make microcapsule with a paraffin core and a SiO_2 wall. They found that the high thermal conductivity of the silica shell improved the thermal properties of PCMs. Al_2O_3 as a mineral with favorable properties such as higher thermal stability, higher thermal conductivity, chemical durability and superior environmental resistance is better in compared with SiO_2 [28]. Fang et al. [29] examined properties and thermal stability and the morphology of aluminum oxide composite based on palmitic acid. Bugaie [30] observed by adding aluminum nanoparticles additive to paraffin could reduce the time of phase change in coolers.

Therefore, considering the importance of microcapsules in energy storage systems, Pourmohamadian et al. [31, 32] prepared two new based palmitic acid (PA) microcapsules with silica dioxide (SiO_2) and strontium titanium ($SrTiO_3$) shells with three shell/core weight ratios (50/50,40/60,30/70). They examined crystalline phase, chemical structure, morphology and thermal properties of composites by using X-ray diffraction (XRD), Fourier transform of infrared spectroscopy (FT-IR), scanning electron microscope (SEM), transmission electron microscope (TEM), differential scanning calorimeter (DSC), and thermal gravimetric analysis (TGA).

This study was carried out using the obtained data of physical properties and using for simulation of thermal process and melting criteria of these materials in energy storing. A rectangular reservoir, containing materials provided under constant heat source were numerically simulated. Transient energy storage results were analyzed for the synthesized microcapsules and compared with the pure palmitic acid (PA).

MODELING

Simulation of porous media has been used in a wide range of issues, such as flow around paper filters, perforated plates, fluid distributors, etc. When one uses the porous medium for simulation, a definite region of the field solution is a porous section with specified values. They create a certain pressure drop in the direction of flow, which can be known by solving the momentum equation in the modified form for the porous medium. Moreover, the heat transfer inside the porous region between the working fluid and the soluble medium can be calculated or ignored. Considering the porous medium, new parameters

such as porosity coefficient, thermal resistance coefficients between the environment and the fluid are added to the solution. This causes the complexity of the solution process and the need to calculate the exact quantities of these parameters with experimental methods for different materials.

Therefore, given that the present problem is conceptually similar to nanofluid issues rather than a porous, assume that there is a non-porous medium with properties related to each simulation section.

The energy equation is considered the main equation for issues that examine the melting and freezing process. The energy equation is considered as:

$$\frac{\partial}{\partial t}(\rho H) + \nabla \cdot (\rho \vec{v} H) = \nabla \cdot (k \nabla T) + S \quad (1)$$

In above equation, H is enthalpy, ρ is the density, k is the thermal conductivity coefficient, *v* is the fluid velocity, and S is the thermal energy source [33]. Here, due to the physical structure of the microcapsules, it is possible to ignore the fluid velocity during the melting process [34,35]. It is possible to break down the total energy of H into two parts of the enthalpy (sensible heat and latent heat) follows:

$$H = h + Lf \quad (2)$$

Here f is the local melting fraction, which is equal to the mass ratio of the melted phase change material to the total mass. The enthalpy of sensible heat is also equal to:

$$h = \int_{T_m}^{T} c \cdot dT \quad (3)$$

For isothermal phase change issues, the local melting fraction is obtained as:

$$f(T) = \begin{cases} 0 & if \quad T < T_{solidus} \\ 1 & if \quad T > T_{liquidus} \\ \frac{T - T_{solidus}}{T_{liquidus} - T_{solidus}} & if \quad T_{solidus} < T < T_{liquidus} \end{cases} \quad (4)$$

By inserting equations (2) and (3) into equation (1) gives:

$$\frac{\partial h}{\partial t} = \frac{k}{\rho}\left(\frac{\partial^2 T}{\partial x^2} + \frac{\partial^2 T}{\partial y^2}\right) - L\frac{\partial f}{\partial t} \quad (5)$$

Equation (5) was discretized using the backward finite difference method and given that, the phase change occurs as homogeneity. Since isothermal phase change occurs, the temperature inside the control volume related to the changing time node is constant and is equal to T_m. Therefore, with respect to equation (5), the value $\frac{\partial h}{\partial t}$ will be zero. In this case, value of f lies between zero and one. The discrete equation was solved using implicit method, which is always stable without the condition. If the volume control is related to the node, which is liquid or frozen, f will be exactly zero or one, respectively. Therefore, $\frac{\partial f}{\partial t}$ will be zero. By solving the equation for each time step in the entire solution range, the temperature and fraction of the melting point were obtained in all nodes. Here the thermal flux boundary condition was considered. The PCM inside a rectangular cavity with the dimensions of 43×38cm was assumed two-dimensional and unsteady. Non-slip boundary condition was applied to each of the four walls. The upper and lower walls were thermally insulated. For the wall on the right with a thermal flux of 600W/m^2 was applied. For the wall on the left a constant temperature of 56°C, equal to the initial temperature of the material was assumed. Figure 1 show a schematic illustration of the problem with applied boundary conditions.

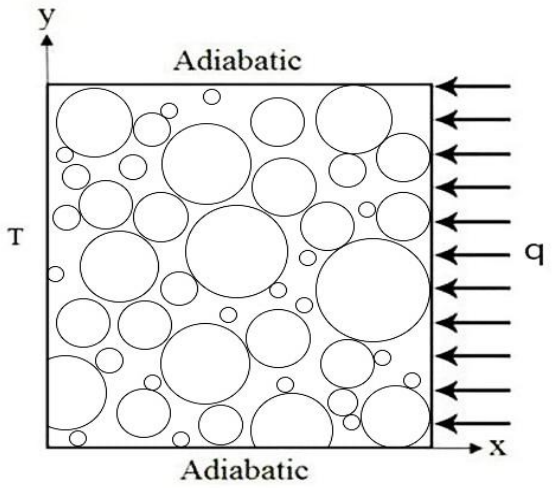


Fig. 1. Solution field and boundary conditions of the problem

The time step was assumed one second with 20 repetitions per time step with the criterion of 0.0001 at each time step. In order to verify the independence of meshing with respect to the results, four different grids size with dimensions of 160×160, 180×180, 200×200, and 220×220 was studied. As shown in Table 1, the 200×200 grid was selected as the acceptable one in terms of accuracy and resolution time . It should be noted that the results are for a distance of 5 mm from the right side of the wall at a time of 4000 seconds. Therefore, each side of this rectangle was divided into 200 nodes and a uniform rectangular grid has been created in the solution medium, which consists of 40401 nodes in the entire solution medium, and this medium has 80400 levels.

Table 1
Independence of the results from networking

Temperature (ºC)	Dimensions
61.6	160×160
63.2	180×180
64.9	200×200
65.6	220×220

The simulation result was compared with the existed analytical solution as presented in the reference [36]. This analytical solution proposed for the simple phase change material with constant thermal conductivity. The boundary conditions and initial condition are similar to this study as follows:

$$T(x,t) = T_l - \frac{qx}{K} + \frac{q^2(x^2+2\propto t)}{2\propto KL\rho} - \frac{q^4(x^4+12\alpha x^2 t+12\alpha^2 t^2)}{12\alpha^3 KL^3\rho^3} \quad (6)$$

The position of the melting front relative to the right side of the wall can be obtained using relation:

$$X(t) = \frac{qt}{L\rho} - \frac{q^3t^2}{2\alpha L^3\rho^3} + \frac{5q^5t^3}{6\alpha^2 L^5\rho^5} \quad (7)$$

Table 2 shows the percent error at different times and points among the analytical solution and the numerical simulation. This shows that as time increased, the error has increased which is due to using fewer terms of the equation and the maximum error of 9.9% has been obtained at 1500 seconds.

Table 2
Comparison between analytic solution and numerical solution

$X(t)$ (mm)	Time=1000s			Time=1150s			Time=1300s			Time=1500s		
	$T_{N.S}$ (°c)	$T_{A.S}$ (°c)	E%	$T_{N.S}$ (°c)	$T_{A.S}$ (°c)	E%	$T_{N.S}$ (°c)	$T_{A.S}$ (°c)	E%	$T_{N.S}$ (°c)	$T_{A.S}$ (°c)	E%
5.8	60.8	61.6	1.3	61.8	64.7	4.5	62.9	67.7	7.1	64.7	71.8	9.9
5.5	61.2	62.2	1.6	62.3	65.3	4.6	63.7	68.4	6.9	65.4	72.5	9.8
5	61.9	63.3	2.2	63.3	66.4	4.7	64.8	69.5	6.8	66.5	73.5	9.5
4	63.8	65.6	2.7	65.1	68.7	5.2	67.1	71.8	6.5	69.1	75.9	8.9
3	65.7	68.1	3.5	66.9	71.2	6	69.3	74.2	6.7	71.5	78.3	8.7

Also, in order to validate the solution process, part of the results of the study by Karimi et al. [37] have been reproduced and compared. They have investigated the heat transfer along with the melting process inside a 3D cavity with dimensions of 43*38*4.5 cm containing solid paraffin. All walls of the cavity except the upper wall are insulated, and the upper wall is under constant heat flux and convective heat transfer with the environment.

Figure 2 shows the temperature versus time graph for the upper wall in the study by Karimi et al.[37] and the results obtained from modeling with the solution method of the present work have also been compared, which has an acceptable correspondence and solution process.

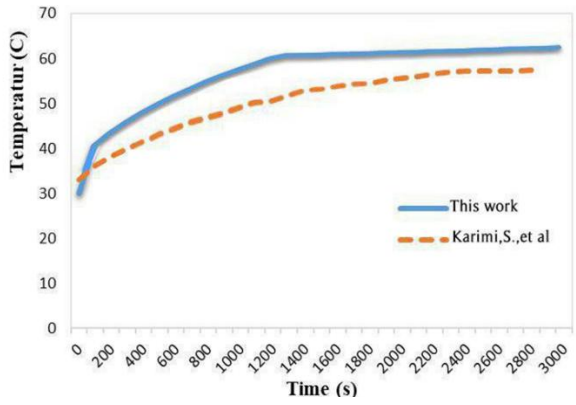


Fig. 2. Comparison of simulated results with those of Karimi et al. [37]

Thermophysical Properties of Microcapsules

The steps for preparing and synthesizing microcapsules are given in the article by Pourmohammadian et al.[31] PA is insoluble in water, and when PA is released in aqueous solution containing surfactant, a stable emulsion of PA / water forms. In this emulsion, the hydrophilic part of the surfactant is in the water phase and away from the organic phase; whereas, the hydrophobic part is located within PA drops. Therefore, a layer of surfactants is formed on the surface of PA drops. On the other hand, Silica-sol (colloidal silanol and its agglomerates) are formed by dissolving sodium silicate in water under the same conditions. When the transparent silica-sol solution is added drop by drop to the PA / water emulsion, silica-sols form a layer on the surface of the surfactant by hydrogen interactions between the hydrophilic surfactant and the hydrolyzed silica. Finally, with the completion of the hydrolysis process, the SiO_2 shell is formed [31].

Then, the thermophilic properties can be obtained from the microcapsules, which are required for thermal simulation.

The corresponding weight fraction ($\emptyset_w$) was obtained for each microcapsule sample from the TGA curves, and then for mixtures/composites with no physical interaction of spherical particles, (ρ_{eff}) effective density, ($\emptyset_v$) volume fraction, and (k_{eff}) effective thermal conductivity coefficient are obtained using following relations [38]:

$$\rho_{eff} = \emptyset_w\rho_c + (1-\emptyset_w) \quad (8)$$

$$\emptyset_v = \frac{\emptyset_w\rho_c}{\emptyset_w\rho_c+(1-\emptyset_w)\rho_d} \quad (9)$$

$$k_{eff} = k_c\left[\frac{k_d+2k_c-2\emptyset_{vd}(k_c-k_d)}{k_d+2k_c+\emptyset_{vd}(k_c-k_d)}\right] \quad (10)$$

Here, the indices of eff, c, and d, are respectively the effective, continuous, and discrete phases, and $\emptyset_{vd}$ is the volume fraction of discrete phase. The specific heat capacity (C_p) is achieved using the DSC curves obtained for each microcapsule sample and follows [39]:

$$C_p = \frac{(dQ/dt)}{(dT/dt)}E \quad (11)$$

In this regard, $\left(dQ/dt\right)$ is the thermal flux in terms of (W/g), $\left(dT/dt\right)$ is the Temperature increase in terms of (◦C / s) and E is the calibration constant of the DSC [31,32].

Table 3 shows the physical properties of the raw materials, PA@SiO_2 microcapsules, and PA@$SrTiO_3$ microcapsules with different weight ratios that were obtained.

Table 3
Physical properties of materials

Materials	Weight Ratio of Core to Shell	Core	Shell	Properties			
		%Øw	%Øv	ρ_{eff} (kg/m^3)	K_{eff} (W/m k)		C_p (J/kg k)
					So	Li	
PA[42]	-	-	-	853	.225	.155	1810
SiO_2[43]	-	-	-	2200	1.38		740
$SrTiO_3$[44]	-	-	-	5120	12		600
PA@SiO_2 [31]	**50/50**	46	75.2	1580.4	.835		1440
	40/60	41	78.78	1647.7	.893		1330
	30/70	34	83.35	1742	.974		1176
PA@$SrTiO_3$ [32]	**50/50**	53	84.2	2858.5	2.86		1312
	40/60	44	88.4	3242.5	3.67		1200
	30/70	38	90.7	3498.5	4.29		1129

RESULTS AND DISCUSSION

The primary phase change material is palmitic acid and other materials are formed on it. Therefore, in this section the results of simulation using palmitic acid as the agent material are presented. Figure 3 shows the variations in the volume fraction of the liquid-solid phase over time. Moreover, Figure 4 depicts the temperature profile for the pure palmitic at three different times of 4000, 8000, and 12000 s.

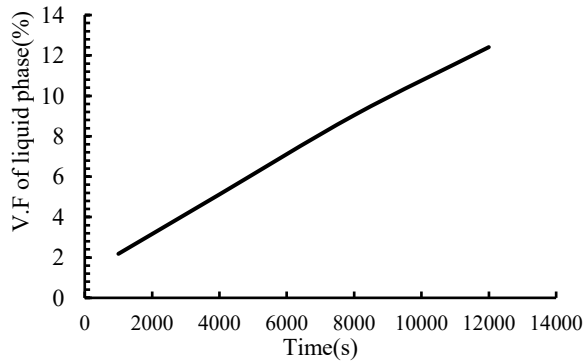


Fig. 3. Volume fraction of the liquid-solid phase of palmitic acid

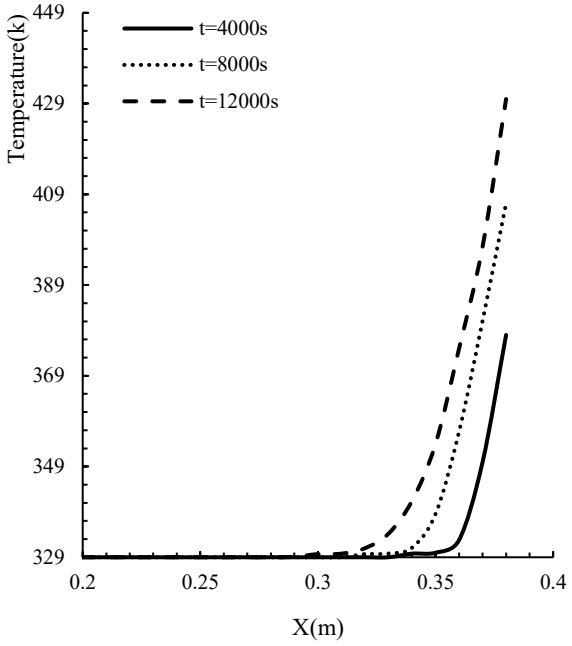


Fig. 4. Temperature profile for pure palmitic acid at different times

In the following, the simulation results using the PA@SiO_2 microcapsule as the agent material were discussed. Figure 5 shows the variations in the volume fraction of the liquid-solid phase relative to time. Moreover, Figure 6 illustrates the temperature profile for PA@SiO_2 with a weight ratio of 50/50, 40/60 and 30/70 at the time of 12000 second.

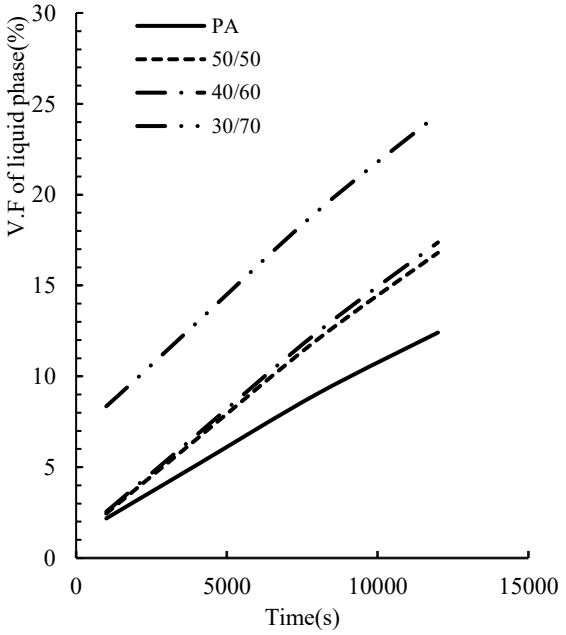


Fig. 5. Volume fraction of the liquid-solid phase of PA@SiO_2 at different weight ratio

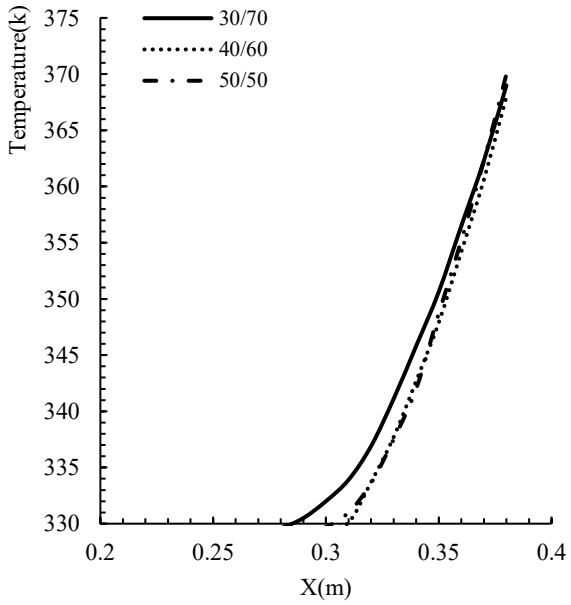


Fig. 6. Temperature profile for PA@SiO_2 with different weight ratios at the time of 12000 s

Now using PA@$SrTiO_3$ as the agent material has been discussed. Figure 7 shows the variations in the volume fraction of the liquid-solid phase relative to time. Moreover, Figure 8 depicts the temperature profile for PA@$SrTiO_3$ with a weight ratio of 50/50, 40/60, and 30/70 at 12000 second.

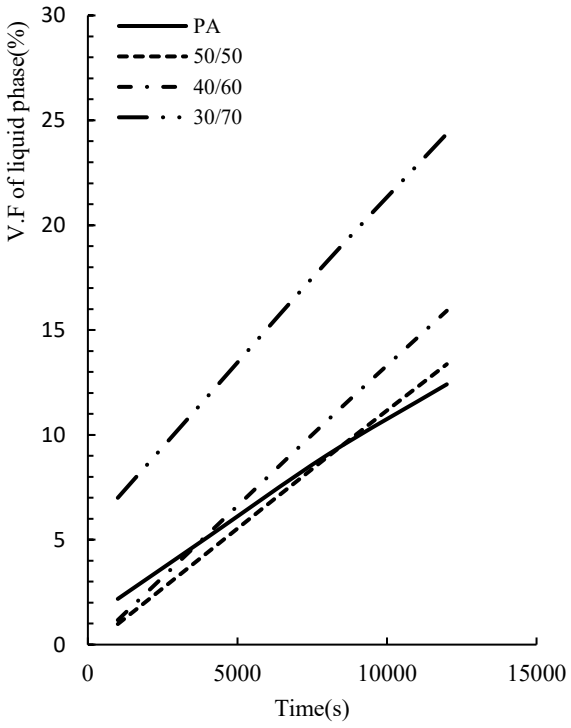


Fig. 7. Volume fraction variations of the liquid-solid phase of PA@ $SrTiO_3$ microcapsules with different weight ratio

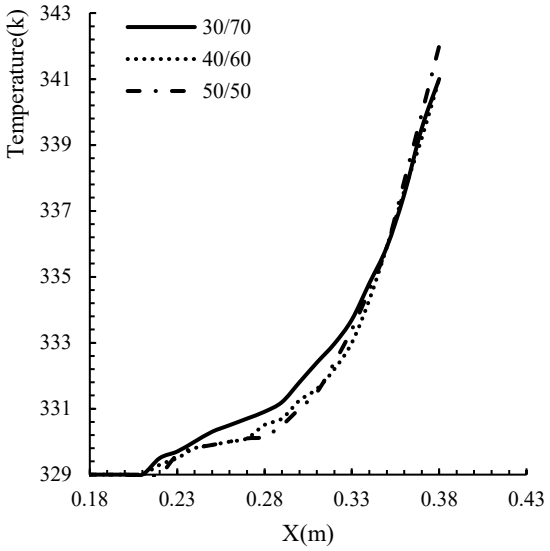


Fig. 8. Temperature profile for PA@ $SrTiO_3$ with different weight ratios at 12000 s

Table 4 compares simulation results of PA, PA@SiO_2 and PA@$SrTiO_3$ microcapsule. As shown in table for PA after 12000 seconds from the beginning of the melting process inside the cavity 12.41% is melted, and 87.59% remained solid. It also indicates that the optimum conditions for PA@SiO_2 microcapsule have a weight ratio of 30/70. After 12000 seconds from the beginning of the melting process inside the cavity, 24.42 % of the melted material and 75.58% of those solid remains, and the maximum temperature is 369 K. Further, it shows that the optimum conditions for PA@ $SrTiO_3$ have a weight ratio of 30/70. After the beginning of the melting process inside the cavity, 24.36% melted and 75.64% of the solid remains and the maximum temperature is 341K.

Table 4
comparison of volume fraction of the liquid phase and the maximum temperature in the solution field for pure PA with PA@SiO_2 and PA@$SrTiO_3$ microcapsules

MATERIALS	Weight Ratio of Core to Shell	Volume Fraction of Liquid Phase (%)			Maximum Temperature (K)		
		4000 s	8000 s	12000 s	4000 s	8000 s	12000 s
PA	-	5.12	9.04	12.41	378	407	430
PA@SiO_2	50/50	6.55	12.02	16.80	348	360	370
	40/60	6.78	12.42	17.37	347	359	368
	30/70	12.95	19.08	24.42	348	360	369
PA@$SrTiO_3$	50/50	4.39	8.94	13.37	336	339	342
	40/60	5.25	10.68	15.92	336	338	341
	30/70	11.83	18.27	24.36	336	339	341

Table 5 shows the results of simulating pure PA and different microcapsules with optimal conditions. As it can be seen, from the various microcapsules, the best results are to be PA@SiO_2 with weight ratio of 30/70 at 12000 second. It has the highest amount of melting volume fraction 24.42%, which has had an increase of 196.8% compared to the pure PA and the maximum wall temperature at this time is 369K.

Table 5
Comparison for optimal microcapsules

MATERIALS	Weight Ratio of Core to Shell	Increase Volume Fraction of Liquid Phase (%)		
		4000s	8000s	12000s
PA@SiO_2	30/70	252.9	211.1	196.8
PA@$SrTiO_3$	30/70	231.1	200.2	196.3

CONCLUSION

In this study, two new types of microcapsules based on palmitic acid (PA) and silica dioxide (SiO_2) and strontium titanium ($SrTiO_3$) with three shell/core weight ratios (50/50, 40/60, 30/70) were prepared and their physical properties were obtained. Then, the thermal process of melting these materials and storing energy in a rectangular reservoir containing constant heat source materials were numerically simulated using the obtained experimental data. The process of transient energy storage for synthesized microcapsules was investigated and analyzed with pure palmitic acid (PA). Among the synthesized microcapsules, the best results are related to PA@SiO_2 with a weight ratio of 30/70. This sample has the highest amount of melting volume fraction 24.42% at the time of 12,000 second, which has increased by up to 196.8% in comparison with the pure PA, and the maximum wall temperature at this time is 369K. According to the results of the simulation of microcapsules, the shell/core is reduced, the thermal latent melting temperature decreases and the thermal conductivity coefficient increases. Therefore, the synthesized microcapsules provide the best results for microcapsules with a weight ratio of 30/70. Consequently, in order to choose the ideal shell/core weight ratio, in addition to considering the results, it is necessary to consider the conditions and purposes for which these materials are to be used.

REFERENCES

[1] Liu C, et al. Experimental study on the thermal performance of capric acid-myristyl alcohol/expanded perlite composite phase change materials for thermal energy storage. Sol Energy. 2019;191:585–95.

[2] Ali HM. Phase change materials based thermal energy storage for solar energy systems. J Build Eng. 2022;56:104731.

[3] Guan Z, Zhang Y. Recent advances in phase change materials for thermal energy storage: A review. Mater Today Energy. 2022;22:100811.

[4] Li Y, Liu Y, Zhang J. Thermal performance of phase change materials in building applications: A review. Energy Rep. 2023;9:1234–45.

[5] Zhang X, Wang Y. A review on the recent developments of phase change materials for thermal energy storage in buildings. Renew Sustain Energy Rev. 2023;169:112511.

[6] Khan MI, Ali S. Phase change materials for energy storage: Recent advancements and future prospects. J Energy Storage. 2022;50:104792.

[7] Sharma R, Kumar V. Innovative phase change materials for building applications: A comprehensive review. Constr Build Mater. 2022;317:125818.

[8] Su W, Darkwa J, Kokogiannakis G. Review of solid–liquid phase change materials and their encapsulation technologies. Renew Sustain Energy Rev. 2015;48:373–91.

[9] Pekarek KJ, Jacob JS, Mathiowitz E. Double-walled polymer microspheres for controlled drug release. Nature. 1994;367:258–60.

[10] Miyazawa K, Yajima I, Kaneda I, Yanaki T. Preparation of a new soft capsule for cosmetics. J Cosmet Sci. 2000;51:239–52.

[11] Hawlader M, Uddin M, Zhu H. Preparation and evaluation of a novel solar storage material: microencapsulated paraffin. Int J Sol Energy. 2000;20:227–38.

[12] Nelson G. Application of microencapsulation in textiles. Int J Pharm. 2002;242:55–62.

[13] Champagne CP, Fustier P. Microencapsulation for the improved delivery of bioactive compounds into foods. Curr Opin Biotechnol. 2007;18:184–90.

[14] Narasimhan NL, Srinivasan G. Analysis of a thermal storage unit containing multiple phase change materials dispersed with high conductivity particles. J Mech Sci Technol. 2018;32(1):373–80.

[15] Kapilow D, Hsuan YG, Sun Y, McCarthy M. Convective melting and freezing of phase change materials encapsulated within small diameter polymer tubes. Exp Therm Fluid Sci. 2018;92:259–69.

[16] Chen ZH, Yu F, Zeng XR, Zhang ZG. Preparation, characterization and thermal properties of nanocapsules containing phase change material n-dodecanol by miniemulsion polymerization with polymerizable emulsifier. Appl Energy. 2012;91:7–12.

[17] Tumirah K, Hussein MZ, Zulkarnain Z, Rafeadah R. Nanoencapsulated organic phase change material based on copolymer nanocomposites for thermal energy storage. Energy. 2014;66:881–90.

[18] Jin Y, Lee W, Musina Z, Ding Y. A one-step method for producing microencapsulated phase change materials. Particuology. 2010;8:588–90.

[19] Yin D, Ma L, Liu J, Zhang Q. Pickering emulsion: A novel template for microencapsulated phase change materials with polymer–silica hybrid shell. Energy. 2014;64:575–81.

[20] Sukhorukov G, Fery A, Möhwald H. Intelligent micro-and nanocapsules. Prog Polym Sci. 2005;30:885–97.

[21] Jamekhorshid A, Sadrameli S, Farid M. A review of microencapsulation methods of phase change materials (PCMs) as a thermal energy storage (TES)

medium. Renew Sustain Energy Rev. 2014;31:531–42.
[22] Castellón C, Martorell I, Cabeza LF, Fernández AI, Manich A. Compatibility of plastic with phase change materials (PCM). Int J Energy Res. 2011;35:765–71.
[23] Giró-Paloma J, Roa J, Díez-Pascual AM, Rayón E, Flores A, Martínez M. Depth-sensing indentation applied to polymers: a comparison between standard methods of analysis in relation to the nature of the materials. Eur Polym J. 2013;49:4047–53.
[24] Kuznik F, David D, Johannes K, Roux JJ. A review on phase change materials integrated in building walls. Renew Sustain Energy Rev. 2011;15:379–91.
[25] Zhou D, Zhao CY. Experimental investigations on heat transfer in phase change materials (PCMs) embedded in porous materials. Appl Therm Eng. 2011;31:970–7.
[26] Wang LY, Tsai PS, Yang YM. Preparation of silica microspheres encapsulating phase-change material by sol-gel method in O/W emulsion. J Microencapsul. 2006;23:3–14.
[27] Zhang H, Wang X, Wu D. Silica encapsulation of n-octadecane via sol–gel process: A novel microencapsulated phase-change material with enhanced thermal conductivity and performance. J Colloid Interface Sci. 2010;343:246–55.
[28] Tang B, Wu C, Qiu M, Zhang X, Zhang S. PEG/SiO2–Al2O3 hybrid form-stable phase change materials with enhanced thermal conductivity. Mater Chem Phys. 2014;144:162–7.
[29] Fang G, Li H, Cao L, Shan F. Preparation and thermal properties of form-stable palmitic acid/active aluminum oxide composites as phase change materials for latent heat storage. Mater Chem Phys. 2012;137:558–64.
[30] Bugaje IM. Enhancing the thermal response of latent heat storage systems. Int J Energy Res. 1997;21:759–66.
[31] Pourmohamadian H, Sheikhzadeh GA, Rahimi-Nasrabadi M, Basirat Tabrizi H. Fabrication and characterization of microencapsulated PA with SiO2 shell through sol–gel synthesis via sodium silicate precursor. J Mater Sci Mater Electron. 2017;28:9990–7.
[32] Pourmohamadian H, Sheikhzadeh GA, Rahimi-Nasrabadi M, Basirat Tabrizi H. Preparation of SrTiO3-microencapsulated palmitic acid by means of a sol–gel approach as thermal energy storage materials. J Mater Sci Mater Electron. 2018;29:794–800.
[33] Bansal NK, Buddhi D. An analytical study of a latent heat storage system in a cylinder. Energy Convers Manag. 1992;33:235–42.
[34] Soma D, Dutta TK. Mathematical modeling and experimental studies on solar energy storage in a phase change material. Sol Energy. 1993;51:305–12.
[35] Murray WD, Landis F. Numerical and machine solutions of transient heat-conduction problems involving melting or freezing. ASME J Heat Transf. 1959;81:106–12.
[36] Maxwell JC. A treatise on electricity and magnetism. Oxford, UK: Clarendon Press; 1873.
[37] Karimi S, et al. Study of phase change modeling for a rectangular PCM container exposed to constant heat flux. Proc WCE. 2013 Jul 3–5; London, UK.
[38] Voller VR. Fast implicit finite-difference method for the analysis of phase change problems. Numer Heat Transf B. 1990;17:155–69.
[39] Ward TL, Singleton WS. Physical properties of fatty acids. II. Some ilatometric and thermal properties of palmitic acid. J Phys Chem. 1952;56(6):696–8.